Airway Closure: Occluding Liquid Bridges in Strongly Buckled Elastic Tubes

Matthias Heil *
DAMTP, University of Cambridge, Cambridge CB3 9EW, U.K.

In print in: ASME Journal of Biomechanical Engineering

Abstract

This paper is concerned with the airway closure problem and investigates the quasi-steady deformation characteristics of strongly collapsed (buckled) airways which are occluded by liquid bridges of high surface tension. The airway wall is modelled as a thin-walled elastic shell which deforms in response to an external pressure and to the compression due to the surface tension of the liquid bridge. The governing equations are solved numerically using physiological parameter values. It is shown that axisymmetric configurations are statically unstable, as are buckled tubes whose opposite walls are not in contact. The quasi-steady deformation characteristics of strongly collapsed airways whose walls are in opposite wall contact show a pronounced hysteresis during the collapse/reopening cycle. Buckling is shown to occur over a short axial length with moderate circumferential wavenumbers. Finally, further implications of the results for the airway collapse/reopening problem are discussed.

1 Introduction

The thin liquid film that lines the airways of the lung can undergo a surface-tension-driven fluid-elastic instability, leading to the formation of liquid bridges across the airway lumen. Evidence for the resulting 'airway closure' has been observed directly (Macklem *et al.* 1970 and Hughes *et al.* 1970) and indirectly (Burger & Macklem 1968 and Otis *et al.* 1996) in experiments on excised animal lungs. Airway closure tends to occur in the smaller airways in the region of the terminal and respiratory bronchioli (Grotberg 1994) and towards the end of expiration when the airway diameters are smallest. This susceptiblity to airway closure is enhanced by diseases which increase the volume of fluid in the lungs (e.g. pulmonary oedema), reduce the structural stiffness of the airways (e.g. emphysema) or increase the surface tension of the liquid lining (e.g. the potentially life-threatening respiratory distress syndrome, frequently experienced by premature neonates). Airway closure is also assumed to contribute to the observed hysteresis in the lung's pressure volume curve (West 1995).

Kamm & Schroter (1989) introduced the concepts of 'film collapse' (airway closure caused by the formation of occluding liquid bridges in an essentially rigid tube) and of 'compliant collapse' (airway closure caused by the surface-tension-dominated compression of the airway walls). Both mechanisms are believed to be important and their interaction was studied by Halpern & Grotberg (1992, 1993), who used a conceptually simple model problem to investigate the liquid bridge formation in an elastic tube. Starting from an initial state in which a uniform liquid film lines a uniform axisymmetric airway, they computed the coupled time-dependent axisymmetric wall and air-liquid interface deformation which follows the initial Rayleigh instability of the liquid lining. They followed the evolution until shortly before the radius of the air-liquid interface approached zero and established that wall elasticity is an important factor in the airway closure problem. The computations predicted axisymmetric wall deformations of up to 20 % of the tube's initial radius. This raises the question of the system's stability to non-axisymmetric perturbations, since thin-walled cylindrical tubes tend to buckle non-axisymmetrically when subjected to strong compressive forces. Motivated by this question, Heil (1999) studied the existence and stability of static liquid bridges in axisymmetric and non-axisymmetrically buckled elastic tubes. The study showed that for physiological parameter values, the axisymmetric configuration is indeed statically unstable and that the compressive load exerted by the liquid bridge on the tube wall is sufficient to induce the tube's buckling. Two possible mechanisms for the formation of occluding liquid bridges in non-axisymmetrically buckled tubes were postulated: In mechanism A, the tube buckles *after* an axisymmetric liquid bridge has been formed – in this case, a relatively large volume of fluid is required to occlude the airway. In mechanism B, the tube buckles during the initial stages of the axisymmetric instability of the liquid lining, i.e. *before* an occluding axisymmetric liquid bridge has been formed – in this case, the minimum volume of fluid required to form an occluding liquid bridge can be significantly smaller.

Heil's (1999) study was restricted to two-lobed buckling modes and to wall shapes without opposite wall contact. However, the stability analysis showed that for physiological values of the parameters, all buckled configurations without opposite wall contact are statically unstable, indicating that only even more strongly collapsed configurations in which the opposing walls have come into contact would be physically realisable.

The present paper is concerned with the quasi-steady deformation characteristics of strongly collapsed elastic tubes which contain liquid bridges of physiologically re-

*New Address: Department of Mathematics, University of Manchester, Manchester M13 9PL, U.K. Email: M.Heil@maths.man.ac.uk.

alistic, high surface tension. It is shown that the static instability of partially collapsed tubes gives rise to hysteresis in the re-opening of the collapsed and occluded airways (which will contribute to the hysteresis in the lung's pressure volume curve) and that high surface tension can lead to buckling deformations with higher circumferential wavenumbers.

2 The Model

Following Heil (1999) we model the partially liquid-filled airway as a thin-walled, linearly elastic tube of diameter R_0, wall thickness h, elastic modulus E and Poisson's ratio ν. The tube contains an occluding liquid bridge enclosed between two air-liquid interfaces of non-dimensional surface tension $\sigma = \sigma^*/(R_0 K)$. The superscript star distinguishes dimensional quantities from their non-dimensional equivalents and $K = E(h/R_0)^3/[12(1-\nu^2)]$ represents the tube's bending stiffness. Lagrangian coordinates $\xi^\alpha = \xi^{*\alpha}/R_0$ are used to parametrise the tube wall such that the vector to the undeformed midplane is given by $\mathbf{r}^0(\xi^\alpha) = \left(\sin(\xi^2), \cos(\xi^2), \xi^1\right)^T$, where $\xi^2 \in [0, 2\pi]$. The deformation displaces the material point on the tube's midplane with coordinates ξ^α to a new position $\mathbf{R}^0(\xi^\alpha) = \mathbf{r}^0(\xi^\alpha) + \mathbf{v}(\xi^\alpha)$ and according to the Kirchhoff-Love assumption, the new position of a material point which was at a distance ξ^3 from the tube's undeformed midplane is given by $\mathbf{R} = \mathbf{R}^0 + \xi^3 \mathbf{N}$, where $\mathbf{N}$ is the unit vector normal to the deformed midplane. The tube is subject to an external pressure $p^*_{ext} = p_{ext} K$ and to the forces due to the surface tension of the liquid bridge. Using the principle of virtual displacements, the tube's deformation is governed by

$$\int\!\!\int \left[E^{\alpha\beta\gamma\delta} \left(\gamma_{\alpha\beta}\ \delta\gamma_{\gamma\delta} + \frac{1}{12}\left(\frac{h}{R_0}\right)^2 \kappa_{\alpha\beta}\ \delta\kappa_{\gamma\delta} \right) - \frac{1}{12(1-\nu^2)}\left(\frac{h}{R_0}\right)^2 (\mathbf{f}\cdot\delta\mathbf{R}) \right] d\xi^1\ d\xi^2 - \int_S \frac{1}{12(1-\nu^2)}\left(\frac{h}{R_0}\right)^2 (\mathbf{l}\cdot\delta\mathbf{R})\, ds = 0, \quad (1)$$

where $\mathbf{f} = \mathbf{f}^*/K$ is the non-dimensional traction per unit area of the undeformed midplane and $\mathbf{l}$ represents a line force (a force per unit length acting along the line S on the inside of the tube). $\gamma_{\alpha\beta}$ and $\kappa_{\alpha\beta}$ are the non-dimensional strain and bending tensors, respectively and $E^{\alpha\beta\gamma\delta} = E^{*\alpha\beta\gamma\delta}/E$ is the dimensionless plane stress stiffness tensor. The summation convention is used and all Greek indices range from 1 to 2. A more detailed discussion of the shell theory can be found in Heil (1999) or Wempner (1973).

Estimates of the Bond number in the small airways (Kamm & Schroter 1989) show that gravity is not important in the problem. Therefore, the two air-liquid interfaces which enclose the liquid bridge are surfaces of constant mean curvature κ, which meet the tube wall at a constant contact angle γ along a contact line whose position has to be determined as part of the solution. We will assume that the contact line can be parametrised in the form $\xi^1 = \xi^1_c(\xi^2)$; see Fig. 1. It should be noted that the system can only be in equilibrium if the wall adjacent to the liquid bridge is considered as dry, otherwise surface-tension-driven draining flows into the liquid bridge persist indefinitely.

We parametrise the meniscus by a set of surface coordinates ζ_α (where $\zeta_1^2 + \zeta_2^2 \le 1$) such that the meniscus shape is given by $\mathbf{R}_m(\zeta_1, \zeta_2)$ and such that the contact line is parametrised by $\varphi = \arctan(\zeta_1/\zeta_2)$. To ensure compatibility with the shell parametrisation we set $\varphi = \xi^2$ and thus obtain the vector to the contact line in terms of the shell displacements as $\mathbf{R}_c(\varphi) = \mathbf{R}(\xi^1 = \xi^1_c(\varphi), \xi^2 = \varphi, \xi^3 = -h/(2R_0))$. The meniscus shape

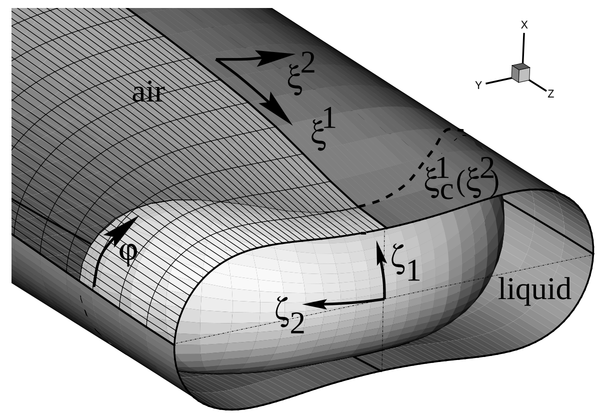

Figure 1: Sketch of the buckled tube containing a meniscus. The ξ^α and ζ_α coordinates parametrise the tube wall and the meniscus, respectively. The contact line is parametrised as $\xi^1 = \xi^1_c(\xi^2)$.

is determined by the principle of virtual displacements (Landau & Lifshitz 1987)

$$\int\!\!\int \left(\delta\sqrt{\mathcal{A}_m} - \kappa\ \mathbf{N}_m \cdot \delta\mathbf{R}_m \sqrt{\mathcal{A}_m} \right) d\zeta_1\ d\zeta_2 = 0. \quad (2)$$

where $\mathcal{A}_m$ is the determinant of the Jacobian of the mapping between the ζ_α-coordinates and the meniscus. The mean curvature of the meniscus $\kappa = \Delta p/\sigma$ is proportional to the pressure jump $\Delta p = \Delta p^*/K$ over the meniscus.

The pressure jump Δp increases the compressive load on the parts of the tube wall which are wetted by the liquid bridge, hence the load terms in (1) are given by

$$\mathbf{f} = \begin{cases} -p_{ext}\mathbf{N} & \text{for} \quad \xi^1 < \xi^1_c(\xi^2) \\ (-p_{ext} - \sigma\kappa)\mathbf{N} & \text{for} \quad \xi^1 \ge \xi^1_c(\xi^2). \end{cases} \quad (3)$$

Note that we have set the reference pressure in the air-filled parts of the tube to zero relative to the external pressure. The line force $\mathbf{l}$ in the variational equation (1) is given by the normal component of the surface tension along the contact line, $\sigma\mathbf{T}\cdot\mathbf{N}$, where $\mathbf{T}$ is the vector normal to the contact line and tangential to the meniscus. Therefore we have

$$\int_S (\mathbf{l}\cdot\delta\mathbf{R})\, ds = \int_0^{2\pi} \left((\sigma\mathbf{T}\cdot\mathbf{N}_w)\mathbf{N}_w \cdot \delta\mathbf{R}_w \right) \left| \frac{\partial \mathbf{R}_c(\varphi)}{\partial\varphi} \right| d\varphi. \quad (4)$$

The lengths of the lung's airways between successive bifurcations is relatively small but for simplicity we will ignore the effects of the bifurcations on the airway deformation. As in Heil (1999), we apply periodic boundary conditions for the wall deformation and set the axial wavelength, λ, to a relatively large value ($\lambda/R_0 = 20$) in order to minimise the direct effect of the boundary conditions on the interaction between the liquid bridge and the wall deformation. We set Poisson's ratio to $\nu = 0.49$ to model the nearly incompressible behaviour of biological tissue and choose a wall thickness of $h/R_0 = 1/20$ which approaches the upper limit of applicability of thin shell theory. Physiologically, the contact angle γ can be expected to be small (or even zero) but as explained in Heil (1999), the case $\gamma = 0$ cannot be studied with the present computational approach. However, it was shown in Heil (1999) that variations in the contact angle only have a small effect on the overall behaviour of the system. For the purpose of the present study we (somewhat arbitrarily) set the contact angle to $\gamma = 10^0$. We also prescribe the dimensionless volume of fluid, $\mathcal{V} = \mathcal{V}^*/R_0^3$, in the liquid bridge. Different values of the surface tension σ and liquid bridge volume $\mathcal{V}$ will be considered in the computations.

These boundary conditions fully specify the problem which was solved numerically by employing finite element discretisations for the wall displacement field, the meniscus shape and the contact line position. Details of the implementation and code validation can be found in Heil (1999). The wall contact problem was implemented by a penalty method (see e.g. Zhong & Mackerle 1992) in which the penalty constant was chosen such that the maximum penetration of the opposite walls was kept below $\mathcal{O}(10^{-3})$.

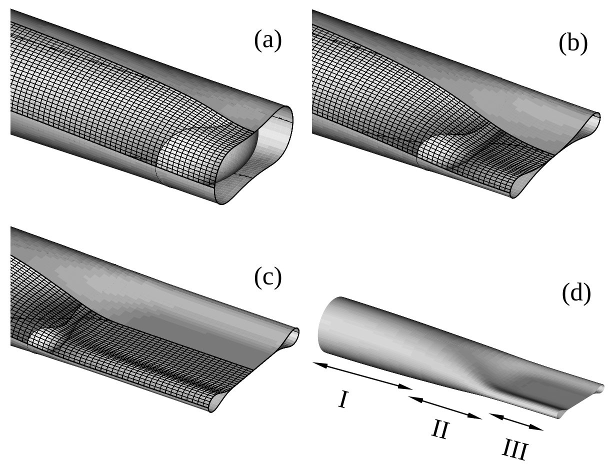

Figure 2: Sequence of increasingly collapsed tubes containing a single liquid bridge ($\mathcal{V} = \mathcal{V}^{(ax.)} = 1.87$, $\sigma = 6$ and $\gamma = 10^0$). The symmetrically deformed tube was cut in the plane of symmetry ($z = 0$) and only one half of the tube and one meniscus are shown. (a)-(c) show the details of the tube's deformation near the liquid bridge, (d) shows the overall deformation. (a) $p_{ext} = -1.11$ (b) $p_{ext} = -4.73$ (c) & (d) $p_{ext} = -3.14$.

3 Results

3.1 Two-lobed collapse

Let us first consider the deformation of an airway in which an occluding axisymmetric liquid bridge has been formed via the mechanism investigated by Halpern & Grotberg (1992, 1993). The liquid bridge exerts a compressive load on the wetted part of the tube wall and the axisymmetric configuration becomes statically unstable when the external pressure is increased beyond a certain critical level. Following the loss of stability the tube buckles non-axisymmetrically and the volume of fluid contained in the liquid bridge is spread out axially.

This is illustrated in Fig. 2, which shows a sequence of increasingly collapsed tubes, containing a single liquid bridge of non-dimensional surface tension $\sigma = 6$. The liquid bridge volume $\mathcal{V}$ was chosen such that it is just sufficient to occlude the airway in the undeformed axisymmetric state ($\mathcal{V} = \mathcal{V}^{(ax.)} = 1.87$ for $\gamma = 10^0$). For these parameter values the axisymmetric configuration first becomes unstable to perturbations with $N = 2$ circumferential waves, leading to a two-lobed collapse. The tube's deformation is symmetric about the plane $z = 0$, therefore in Fig. 2 the tube was cut in the plane of symmetry and only one half of the tube and one meniscus are shown. As the tube's collapse increases, the shape of the most strongly collapsed cross section changes from elliptical to dumbbell shaped (Fig. 2a). In Fig. 2b, the tube is so strongly collapsed that opposite wall contact occurs for the first time (in point contact on the tube's centreline). A further increase in collapse establishes opposite wall contact over an increasing length of the tube. The corresponding reduction in lumen forces the air-liquid interface to move far

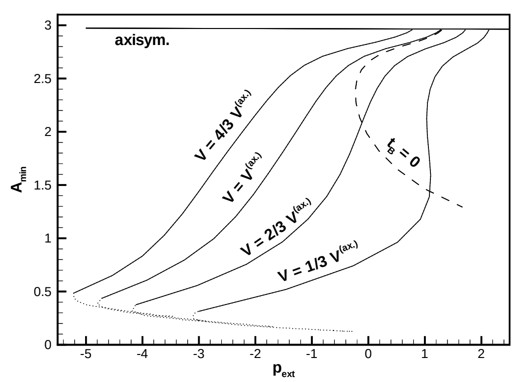

Figure 3: Deformation characteristics for tubes containing liquid bridges ($\sigma = 6$, $\gamma = 10^0$) of various volumes $\mathcal{V}$. The tubes buckle in a two-lobed mode. The dotted and solid lines represent configurations with and without opposite wall contact, respectively. The dashed line corresponds to liquid bridges of zero thickness. All points to its right represent physically unrealisable configurations in which the two menisci intersect. $\mathcal{V}^{(ax.)} = 1.87$.

along the tube since the volume of fluid contained in the liquid bridge has to be conserved. Away from the meniscus, the tube quickly reopens to its original axisymmetric shape. This allows the strongly collapsed tube to be subdivided into three main regions which are distinguished by their local degree of collapse (I: uniformly inflated, II: transition, III: uniformly collapsed; see Fig. 2d). The transition region II over which the tube reopens has an axial length of a few tube radii.

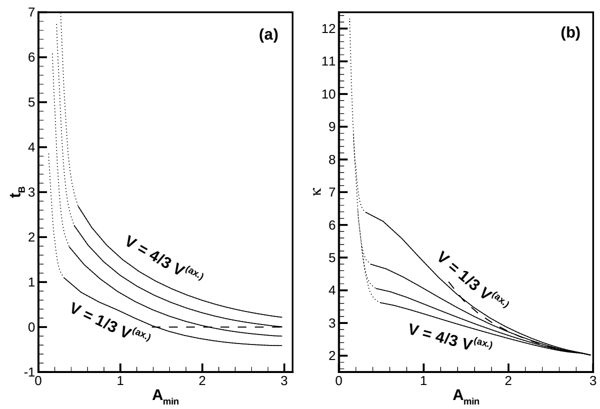

Figure 4: Liquid bridge thickness t_b and meniscus curvature κ for liquid bridges ($\sigma = 6$, $\gamma = 10^0$) of various volumes, $\mathcal{V} = 1/3\mathcal{V}^{(ax.)}, 2/3\mathcal{V}^{(ax.)}, \mathcal{V}^{(ax.)}$ and $4/3\mathcal{V}^{(ax.)}$. The dotted and solid lines represent configurations with and without opposite wall contact, respectively. The dashed line corresponds to liquid bridges of zero thickness.

In Fig. 3 the corresponding deformation characteristics are illustrated by plotting the tube's cross sectional area in the plane of symmetry, $\mathcal{A}_{min}$, versus the external pressure. Different curves correspond to different liquid bridge volumes $\mathcal{V}$. Let us first consider the case $\mathcal{V} = \mathcal{V}^{(ax.)}$, which was illustrated in Fig. 2. For large negative values of the external pressure, the tube is inflated throughout its length and deforms axisymmetrically. Axisymmetric deformations are accompanied by circumferential stretching of the tube wall and in this mode the tube is very stiff: Large changes in external pressure are required to change the tube's cross sectional area. This manifests itself in the small negative slope of the nearly straight line which corresponds to the axisymmetric state. As the external pressure is increased, the tube first becomes compressed in the region which is wetted by the liquid bridge and for $p_{ext} = p_{ext}^{(coll.)} = 1.28$ the compression is so strong that the axisymmetric state becomes unstable. The tube's initial post-buckling deformation is described by the backward facing curve which emanates from the buckling point. The fact that the curve is backward facing reflects the static instability of the partially collapsed configuration, as discussed in detail in Heil (1999). In this unstable regime, a decrease in external pressure would be required to monotonically increase the tube's collapse. In an experiment, the loss of axisymmetric stability would be followed by a large (dynamic) jump into a strongly collapsed configuration with opposite wall contact. The occurrence of opposite wall contact is marked by a change in linestyle from solid to dotted. Fig. 3 shows that the occurrence of opposite wall contact rapidly increases the tube's stiffness to such an extent that the restoring elastic forces are sufficient to stably balance the compressive load exerted by the liquid bridge: An increase in external pressure is required to further increase the tube's collapse.

Note that the static instability of the partially collapsed tubes gives rise to a pronounced hysteresis loop: If the strongly collapsed tube is reopened (by decreasing the external pressure) it will (dynamically) jump back into the axisymmetric configuration when the external pressure is reduced below $p_{ext} = p_{ext}^{(reop.)} = -4.80$ which is substantially smaller than the pressure $p_{ext}^{(coll.)}$ at which the axisymmetric tube collapsed.

Figs. 4a,b illustrate how the liquid bridge thickness t_B (defined as the minimal axial distance between the two air-liquid interfaces) and the meniscus curvature κ vary with the tube's collapse. The constant volume constraint results in an increase in t_B as $\mathcal{A}_{min}$ is reduced. In a strongly collapsed tube, a large fraction of the liquid bridge volume is contained in the two outer lobes of the uniformly collapsed region III whose cross sectional area is given by $\mathcal{A}_{min}$. Hence, in this regime, t_B varies approximately inversely with the cross sectional area $\mathcal{A}_{min}$ and grows very rapidly with increasing collapse. As the meniscus moves further into the tube, the length of region III also increases and the apex of the wall contact region approaches the meniscus (see Fig. 2c). This reduces the vertical width of the gap between the walls enclosing the meniscus and causes rapid growth of the meniscus curvature κ. For strongly collapsed tubes, κ becomes so large that the pressure jump over the meniscus, $\Delta p = \sigma\kappa$, provides the main contribution to the compressive load on the wetted part of the tube wall. This explains why only a relatively small increase in external pressure is required to achieve large changes in $\mathcal{A}_{min}$ even in a regime in which large parts of the tube wall are in opposite wall contact and in which the tube has regained a very high stiffness. For instance, for $\mathcal{V} = 1/3\ \mathcal{V}^{(ax.)}$ a reduction of the cross sectional area from $\mathcal{A}_{min} = 0.231$ to $\mathcal{A}_{min} = 0.125$ requires an increase in the total compressive load on the wetted part of the tube wall from $|\mathbf{f}| = 38.6$ to $|\mathbf{f}| = 73.57$. Fig. 3 shows that this achieved by a comparatively small increase in external pressure from $p_{ext} = -3.00$ to $p_{ext} = -0.29$.

The other curves in Figs. 3 and 4 illustrate the effect of variations in liquid bridge volume $\mathcal{V}$. We will now discuss the effect of such variations on the tube's stability and on the deformation characteristics of moderately and strongly collapsed tubes.

Let us first consider the stability of the axisymmetric configuration: An increase in fluid volume increases the thickness t_B of the liquid bridge (see Fig. 4a). The corresponding increase in wetted wall area increases the compressive load on the axisymmetric tube, hence a smaller external pressure is required to induce buckling. Similarly, a reduction in liquid bridge volume would increase the buckling pressure. However, for $\mathcal{V} < \mathcal{V}^{(ax.)}$, the fluid volume is not sufficient to form an occluding liquid bridge in the axisymmetric tube. Occluding liquid bridges of such small volume can only have been formed via mechanism B. As the tube is re-opened, the two air-liquid interfaces approach each other and come into contact at the position indicated by the dashed lines which represent states for which $t_B = 0$. Further re-opening of the tube destroys the liquid bridge. The data points to the right of the dashed line in Fig. 3 correspond to hypothetical configurations in which the two air-liquid interfaces intersect.

Figs. 5a,b illustrate the effect of variations in $\mathcal{V}$ on the deformation of moderately collapsed tubes. For a given degree of collapse (first opposite wall contact) a reduction in $\mathcal{V}$ has two effects. First, the meniscus curvature increases (see also Fig. 4b) since the meniscus moves closer to the most strongly collapsed cross section. Second, since the tube is wetted (and hence compressed) over a shorter length, the axial bending moments are increased. Figs. 5a,b show that this reduces the cross sectional area $\mathcal{A}_{min}$ in the plane of symmetry. This can also be seen in Fig. 3: For increased fluid volume the first opposite wall contact occurs at larger values of $\mathcal{A}_{min}$.

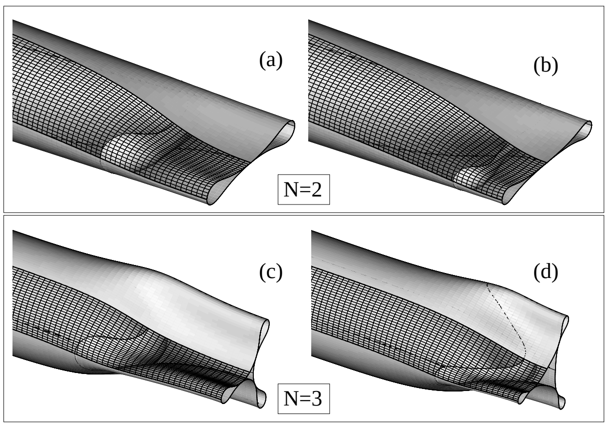

Figure 5: Illustration of the effect of variations in liquid bridge volume $\mathcal{V}$ on moderately collapsed tubes in first opposite wall contact. (a) and (c): $\mathcal{V} = 4/3\ \mathcal{V}^{(ax.)}$, (b) and (d): $\mathcal{V} = 1/3\ \mathcal{V}^{(ax.)}$. (a) and (b): $\sigma = 6$, (c) and (d): $\sigma = 25$. $\gamma = 10^0$.

Finally, for strongly collapsed tubes in which the three regions, identified in Fig. 2d, are fully established, the main effect of an increase in $\mathcal{V}$ is an increase in the axial length of region III; the shapes of regions I and II (and hence the meniscus curvature κ) become independent of $\mathcal{V}$. This is demonstrated in Figs. 6a,b which show horizontal and vertical sections through the axial planes of symmetry in two strongly collapsed tubes which contain liquid bridges of different volume ($\mathcal{V} = 1/3\ \mathcal{V}^{(ax.)}$ and $2/3\ \mathcal{V}^{(ax.)}$). The solid lines represent the respective wall and meniscus shapes; the dashed lines (which can only be distinguished from the solid lines near the left end of the domain) were generated by shifting the wall and meniscus shapes corresponding to $\mathcal{V} = 1/3\ \mathcal{V}^{(ax.)}$ to the left (by $\Delta z = -1.81$) in order to overlay them with those corresponding to $\mathcal{V} = 2/3\ \mathcal{V}^{(ax.)}$. The small deviations near the left end of the domain correspond to weak end effects which indicate that the wavelength of the periodic deformation was not long enough to eliminate the influence of the boundary conditions completely.

As discussed above, in such strongly collapsed tubes the meniscus curvature has increased to such an extent that the compressive load on the wetted part of the tube is dominated by the pressure jump over the meniscus ($\Delta p = \sigma\kappa = 51.96$ compared to $p_{ext} \approx -2$). Hence, the curves $\mathcal{A}_{min}(p_{ext})$ in Fig. 3 all approach the same slope as the tube's collapse increases since the meniscus curvature becomes independent of $\mathcal{V}$.

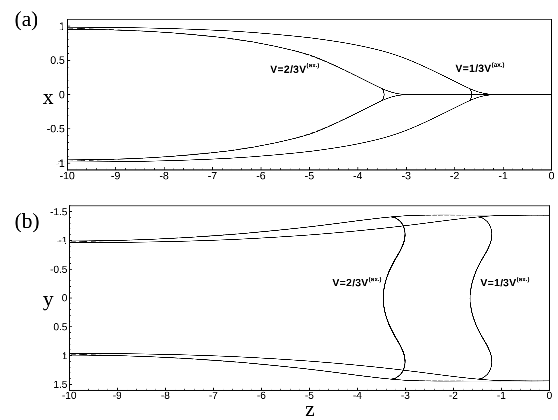

Figure 6: Vertical (a) and horizontal (b) axial sections through the planes of symmetry of two strongly collapsed tubes of different liquid bridge volume $\mathcal{V}$. The solid lines show the wall and meniscus shapes. The barely noticeable dashed line was created by overlaying the wall and meniscus shapes for the two cases. $p_{ext} = -1.96$ for $\mathcal{V} = 1/3\mathcal{V}^{(ax.)}$ and $p_{ext} = -1.78$ for $\mathcal{V} = 2/3\mathcal{V}^{(ax.)}$. $\sigma = 6$, $\gamma = 10^0, \kappa = 8.66, \mathcal{A}_{min} = 0.173$ for both cases.

3.2 Three-lobed collapse

Thus far we have only considered tubes which collapse in a two-lobed mode. In Heil (1999) this was motivated by previous investigations into airway reopening (Gaver *et al.* 1990) in which the collapsed airways had been assumed to have buckled in this mode. The assumption of a two-lobed collapse is justified for liquid bridges of relatively low surface tension since the initial stages of their collapse are dominated by the external pressure, p_{ext}, which is applied uniformly over the length of the tube. In this case, the entire length of the tube participates in the buckling and computational studies show that the axisymmetric state first becomes unstable to non-axisymmetric perturbations with $N = 2$ circumferential waves when p_{ext} is increased slowly.

As the surface tension is increased, the tube's compression becomes dominated by the load caused by the liquid bridge which only acts over a short axial length. Hence the fraction of the tube's length over which buckling occurs is reduced and the collapsing part of the tube behaves like a shorter tube which is supported between fairly stiff supports (provided by the parts of the tube which do not participate in the buckling). It is well known that shorter cylindrical tubes buckle with higher circumferential wavenumbers (Yamaki 1984), therefore we might expect an increase in surface tension to result in an increase in the most unstable circumferential wavenumber.

Computational investigations confirm that this transition does indeed occur and an example of a tube collapsing in a three-lobed mode is shown in Fig. 7. This tube contains a liquid bridge of non-dimensional surface tension $\sigma = 25$. For this surface tension, the axisymmetric configuration loses its stability to perturbations with $N = 3$ circumferential waves when p_{ext} exceeds a value of $p_{ext}^{(coll.)} = -21.01$ (see Fig. 8). Note that for such large surface tensions, buckling is initiated by the liquid bridge alone: when the tube buckles, the dry parts of the tube wall are still subject to a large positive transmural pressure.

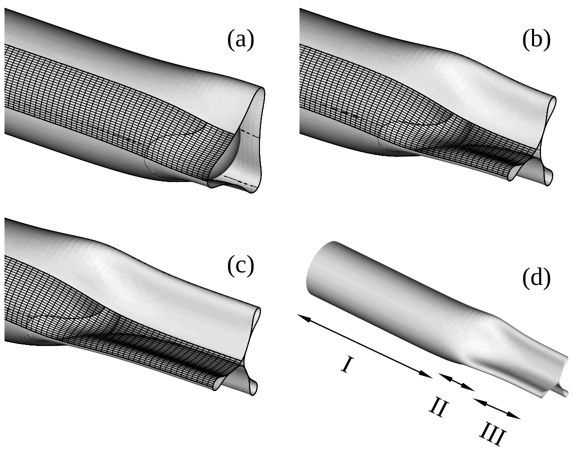

Figure 7: Sequence of increasingly collapsed tubes which have buckled in a three-lobed mode. The symmetrically deformed tube was cut in the plane of symmetry ($z = 0$) and only one half of the tube and one meniscus are shown. (a)-(c) show the details of the tube's deformation near the liquid bridge, (d) shows the overall deformation. (a) $p_{ext} = -19.51$ (b) $p_{ext} = -33.17$ (c) & (d) $p_{ext} = -29.31$. $\mathcal{V} = \mathcal{V}^{(ax.)} = 1.87$, $\sigma = 25$ and $\gamma = 10^0$.

The tube's deformation shows some features which are quite distinct from those seen in the two-lobed collapse in Fig. 2, but fairly generic for all buckling modes with higher wavenumbers. First opposite wall contact occurs simultaneously at multiple points and the central part of the tube's cross section remains open throughout its deformation. The large wall curvature in the outer lobes makes the contact line 'rise' more strongly than in the two-lobed case in which there was less circumferential variation of the axial contact line position. The large pressure jump over the meniscus (mainly caused by the larger surface tension) leads to sharp transition between the collapsed and inflated parts of the tube. The length of the transition region II is mainly determined by the axial extent of the meniscus.

As in the the two-lobed case, a three region pattern is formed when opposite wall contact is established over a sufficient axial length of the tube. The tube's deformation characteristics in Fig. 8 show that after an initial moderate snap through, which follows the loss of axisymmetric stability, the larger bending moments generated in a three-lobed collapse are sufficient to stabilise the tube in a moderately collapsed state without opposite wall contact. However, a further increase in external pressure (and collapse), increases the meniscus curvature (and hence the pressure jump over the meniscus) so rapidly that this moderately collapsed state also becomes unstable. This manifests itself in the limit point in the deformation characteristics at about $\mathcal{A}_{min} \approx 1.6$. An increase in external pressure beyond the limit point ($p_{ext}^{(lim.)} = -18.10$ for $\mathcal{V} = \mathcal{V}^{(ax.)}$) renders the tube unstable: In an experiment it would dynamically collapse into a more strongly collapsed configuration with opposite wall contact.

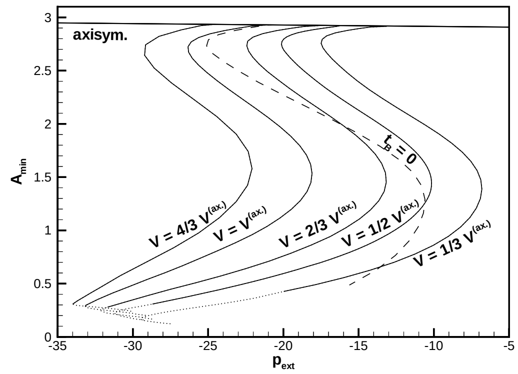

Figure 8: Deformation characteristics for tubes containing liquid bridges ($\sigma = 25$, $\gamma = 10^0$) of various volumes $\mathcal{V}$. The tubes buckle in a three-lobed mode. The dotted and solid lines represent configurations with and without opposite wall contact, respectively. The dashed line corresponds to liquid bridges of zero thickness. All points to its right represent physically unrealisable configurations in which the two menisci intersect.

The occurrence of opposite wall contact is again indicated by a change in linestyle and Fig. 8 shows that for smaller liquid bridge volumes, the occurrence of opposite wall contact does not stabilise the tube as quickly as it does for liquid bridges of larger volume. The reason for this becomes apparent from Figs. 5c,d which show two tubes which contain liquid bridges of different volumes ($\mathcal{V} = 1/3\ \mathcal{V}^{(ax.)}$ and $4/3\ \mathcal{V}^{(ax.)}$). For both tubes opposite wall contact has just occured for the first time. For the tube which contains the larger volume of fluid (Fig. 5c), the meniscus has already moved far from the plane of symmetry which is therefore virtually unaffected by the circumferential variations in the contact line position. Conversely, in the tube with the smaller liquid bridge volume (Fig. 5d) the contact line position has a noticeable effect on local deformation: Whereas the outer lobes are already strongly compressed over a significant axial length, the central part of the tube is held open by the large positive transmural pressure in the closely adjacent dry parts of the wall. Hence the wall shape is markedly different from the final stable configuration in which the meniscus has moved further into the tube and a zone of axially uniform collapse has developed. As in the two-lobed case the development of the uniformly collapsed region III manifests itself in the identical slopes of the $\mathcal{A}_{min}(p_{ext})$ curves for all meniscus volumes.

4 Discussion

We shall now discuss the implications and relevance of the above results for the airway closure problem. The most important parameter identified in the present study is the non-dimensional surface tension $\sigma = \sigma^*/(R_0 K)$ which represents the ratio of the typical pressure jump over the meniscus to the tube's bending stiffness. Many of the parameters affecting its value are only known approximately and a wide range of values has been used by different authors. Estimates for the airway's elastic modulus range from $E = 6kPa$ (Halpern & Grotberg 1992, 1993) to $E = 20kPa$ (Hill *et al.* 1997). The presence of surfactant can reduce the surface tension of an uncontaminated interface from $\sigma^* \approx 2 \times 10^{-2} N/m$ to $1 \times 10^{-2} N/m$ and less. A further important factor is the radius of the airways which depends on the exact location of the liquid bridge (Weibel & Gomez 1962). For a thickness-to-radius ratio of $h/R_0 = 1/10$ (as in Halpern & Grotberg 1992, 1993 – recent measurements by Riess *et al.* 1996 suggest somewhat larger values) these variations correspond to a range of non-dimensional surface tensions between $\sigma = 6$ (for $R_0 = 0.75mm, E = 20kPa$ and $\sigma^* = 1 \times 10^{-2} N/m$) to $\sigma = 120$ (for $R_0 = 0.25mm, E = 6kPa$ and $\sigma^* = 2 \times 10^{-2} N/m$). The values used in the above computations were chosen in the lower part of this range – mainly because larger values of σ would lead to pre-buckling deformations which are too large to justify the small strain assumption used in the constitutive model for the airway wall. Nevertheless, it is interesting to note that even for the most conservative estimate of σ, we found the axisymmetric configuration to be strongly unstable to non-axisymmetric perturbations.

We have only considered the system's response to quasi-steady changes in external pressure. This is only legitimate if the system adjusts itself to such changes over a timescale $\Delta\tau$ which is shorter than the duration of one breathing cycle. Hill *et al.*(1997) estimated the viscous timescale for the redistribution of the fluid in a thin liquid film inside an elastic tube to be $\Delta\tau \approx \mathcal{O}(0.1sec)$ and thus showed that a quasi-steady analysis is justified in their problem. We expect similar or even shorter timescales to apply to the viscous dynamics of liquid bridges in moderately collapsed tubes since the dimensions of liquid bridges are larger than those of the thin liquid films considered in their study. However, in strongly collapsed tubes the flow resistance in the narrow outer lobes and in the squeeze film that will develop between the two opposite walls when they approach each other will be significant. In this case the timescales required to reopen the collapsed tube could be drastically increased and the reopening process would be governed by mechanisms similar to those studied by Gaver *et al.* (1990) and Gaver *et al.* (1996). While the quasi-steady analysis identifies the equilibrium states at either end of the snap-through closing and reopening, it cannot provide any insight into the complicated fluid-structure interaction during the dynamic transition between these states. The most serious shortcoming of the present model presumably lies in the neglect of the parenchymal tethering which would contribute to the system's stiffness and has previously been shown to play a role in the airway reopening problem (Yap *et al.* 1994). In order to obtain a simple mechanical model we have only analysed liquid bridges in tubes whose length is larger than the typical distance between successive airway bifurcations. However, since the airway collapse was found to be restricted to a short axial length, we do not expect the results to be significantly affected by a reduction of the tube's length or by the application of different boundary conditions for the tube's deformation.

Further computations which investigated the effects of axial wall tension and of variations in the contact angle were performed but the results were not included in this paper since neither changed the results qualitatively. Increased axial tension had the two obvious effects of (i) stabilising the axisymmetric state slightly and (ii) making the tube's deformation more smooth, resulting in an increase in the length of the transition region II.

We have shown that large surface tension leads to a strongly localised compression of the airways which favours a collapse with a higher number of circumferential waves. This is in agreement with observations (Hughes *et al.* 1970) which show that airway closure occurs over a relatively short axial length with a moderate number of circumferential waves. Note that this effect is complementary to the increase in wavenumber caused by the presence of parenchymal tethering (Wang *et al.* 1983).

The hysteresis in the deformation characteristics caused by the instability of the partially collapsed configurations has interesting implications for observations made in the airway re-opening studies by Burger & Macklem (1968) and Otis *et al.* (1996). They (and other authors) found that the open airways close when subjected to a compressive (negative) transmural pressure but only reopen when the transmural pressure is increased to larger positive value. Burger & Macklem (1968) speculated that the positive re-opening pressure was required to overcome the compression caused by an occluding liquid bridge. They postulated a relatively large surface tension (of $\sigma = 5 \times 10^{-2} N/m$) since they assumed that the compression was generated by the pressure jump over two axisymmetric menisci. The results presented here suggest a slightly different explanation for the reported observations: If an axisymmetric liquid bridge has been formed in an airway (via mechanism A) then the subsequent non-axisymmetric collapse of the occluded airway increases the meniscus curvature significantly (see Fig. 4b) and thus provides a much stronger compressive load than estimates based on the axisymmetric configurations would suggest. Reopening of the collapsed airway (to an axisymmetric state) will then occur when the external pressure has been reduced to $p_{ext}^{(reop.)} \approx -\sigma\kappa^{(reop.)}$. Since $\kappa^{(reop.)}$ is several times larger than the meniscus curvature in an axisymmetric tube, Burger & Macklem's (1968) observations can be explained with more realistic values for the surface tension.

In this context it should also be noted that reopening to an axisymmetric state is not equivalent to the removal of the occlusion as is tacitly implied in Burger & Macklem's (1968) argument. Even if the airway was axisymmetric, an occluding liquid bridge would persist even for $p_{ext} < p_{ext}^{(reop.)}$. The liquid bridge would only be destroyed if the airway was inflated to such an extent that the constant volume constraint forced the two menisci which enclose the liquid bridge to come into contact. Only occluding liquid bridges which were formed via mechanism B and whose volume is smaller than the volume required to form an occluding liquid bridge in the axisymmetric tube, are destroyed by the sudden reopening that occurs when $p_{ext} < p_{ext}^{(reop.)}$.

5 Summary

We have studied the quasi-steady deformation characteristics of strongly buckled elastic tubes which contain a liquid bridge of large non-dimensional surface tension and interpreted the results in the context of the airway closure problem. We showed that the instability of the partially collapsed configurations (without opposite wall contact) gives rise to a pronounced hysteresis loop in a collapse/reopening cycle. Thus, we have identified a new mechanism which contributes to the hysteresis in the lung's pressure volume curve. It was shown that for physiological parameter values, buckling will occur over a short axial length and with a moderately large circumferential wavenumber. The mechanism for the increase in the circumferential wavenumber is complementary to the effects of parenchymal tethering (which was neglected in this study) and is consistent with experimental observations of airway closure.

Acknowledgements

The author wishes to thank Prof. T.J. Pedley, Dr. Oliver Jensen, Dr. Harvey Williams, Dr. Naomi Chesler and Dr. Andrew Hazel for many fruitful and enjoyable discussions. Financial support for this research was provided by the EPSRC.

References

Burger, E.J. & Macklem, P. 1968 Airway Closure: Demonstration by Breathing 100 % O_2 at Low Lung Volumes and by N_2 Washout. Journal of Applied Physiology **25**, 139-148.

Gaver, D.P. III, Halpern, D. Jensen, O.E. & Grotberg, J. 1996 The steady motion of a semi-infinite bubble through a flexible walled channel. Journal of Fluid Mechanics **319**, 25-56.

Gaver, D.P. III, Samsel, R.W. & Solway, J. 1990 Effects of Surface Tension and Viscosity on Airway Reopening. Journal of Applied Physiology **69**, 74-85.

Grotberg, J.B. 1994 Pulmonary Flow and Transport Phenomena. Annual Review of Fluid Mechanics **26**, 529-571.

Halpern, D., Grotberg, J.B. 1992 Fluid-Elastic Instabilities of Liquid-Lined Flexible Tubes. Journal of Fluid Mechanics **244**, 615-632.

Halpern, D., Grotberg, J.B. 1993 Surfactant Effects on Fluid-Elastic Instabilities of Liquid-Lined Flexible Tubes: A Model of Airway closure. ASME Journal of Biomechanical Engineering **115**, 271-277.

Heil, M. 1999 Minimal Liquid Bridges in Non-Axisymmetrically Buckled Tubes. Journal of Fluid Mechanics **380**,309-337.

Hill, M.J., Wilson, T.A. & Lambert, R.K. 1997 Effect of Surface Tension and Intraluminal Fluid on Mechanics of Small Airways. Journal of Applied Physiology **82**, 233-239.

Hughes, J.M.B., Rosenzweig, D.Y. & Kivitz, P.B. 1970 Site of Airway Closure in Excised Dog Lungs: Histologic Demonstration. Journal of Applied Physiology **29**, 340-344.

Kamm, R.D. & Schroter 1989 Is Airway Closure Caused by a Liquid Film Instability? Respiration Physiology **75**, 141-156.

Landau, L.D. & Lifshitz, E.M. 1987 Fluid Mechanics. Pergamon Press, Oxford.

Macklem, P.T., Proctor, D.F. & Hogg, J.C. 1970 The Stability of the Peripheral Airways. Respiration Physiology **8**, 191-203.

Otis, D.R., Petak, F., Hantos, Z., Fredberg, J.J. & Kamm, R.D. 1996 Airway Closure and Reopening Assessed by the Alveolar Capsule Oscillation Technique. Journal of Applied Physiology **80**, 2077-2084.

Riess, A., Wiggs, B., Verburgt, L., Wright, J.L., Hogg, J.C. & Paré, P.D. 1996 Morphologic Determinants of Airway Responsiveness in Chronic Smokers. American Journal of Respiratory and Critical Care Medicine **154**, 1444-1449.

Wang, C.Y., Watson, L.T. & Kamat, M.P. 1983 Buckling, Postbuckling and the Flow Through a Tethered Elastic Cylinder Under External Pressure. ASME Journal of Applied Mechanics **50**, 13-18.

Weibel, E.R. & Gomez, D.M. 1962 Architecture of the Human Lung. Science **137**, 577-585.

Wempner, G. 1973 Mechanics of Solids. McGraw-Hill, New York.

West, J.B. 1995 Respiratory Physiology – the Essentials. 5th edition. Williams & Wilkins, Baltimore.

Yamaki, N. 1984 Elastic Stability of Circular Cylindrical Shells. North-Holland, Amsterdam.

Yap, D.Y.K., Liebkemann, W.D., Solway, J. & Gaver, D.P. 1994 The Influence of Parenchymal Tethering on the Reopening of Closed Pulmonary Airways. Journal of Applied Physiology **76**, 2095-2105.

Zhong, Z.-H.& Mackerle, J. 1992 Static Contact Problems - A Review. Engineering Computations **9**, 3-37.